**SANDIA REPORT**
SAND2012-6138
Unlimited Release
Printed September 2012

# Ion-Photon Quantum Interface: Entanglement Engineering

David L. Moehring, Jonathan D. Sterk, Francisco Benito, and Matthew G. Blain

Prepared by David L. Moehring
Sandia National Laboratories
Albuquerque, New Mexico 87185

Sandia National Laboratories is a multi-program laboratory managed and operated by Sandia Corporation, a wholly owned subsidiary of Lockheed Martin Corporation, for the U.S. Department of Energy's National Nuclear Security Administration under contract DE-AC04-94AL85000.



Issued by Sandia National Laboratories, operated for the United States Department of Energy by Sandia Corporation.



Available to DOE and DOE contractors from
U.S. Department of Energy
Office of Scientific and Technical Information
P.O. Box 62
Oak Ridge, TN 37831

Telephone: (865) 576-8401
Facsimile: (865) 576-5728
E-Mail: reports@adonis.osti.gov
Online ordering: http://www.osti.gov/bridge

Available to the public from
U.S. Department of Commerce
National Technical Information Service
5285 Port Royal Rd.
Springfield, VA 22161

Telephone: (800) 553-6847
Facsimile: (703) 605-6900
E-Mail: orders@ntis.fedworld.gov
Online order: http://www.ntis.gov/help/ordermethods.asp?loc=7-4-0#online

SAND2012-6138
Unlimited Release
Printed September 2012

# Ion-Photon Quantum Interface: Entanglement Engineering

David L. Moehring, Jonathan D. Sterk, Francisco Benito, and Matthew G. Blain
Photonic Microsystem Technologies
Sandia National Laboratories
P.O. Box 5800
Albuquerque, New Mexico 87185-MS1082

**Abstract**

Distributed quantum information processing requires a reliable quantum memory and a faithful carrier of quantum information. Trapped ion qubits are the leading realization for quantum information storage, and photonic qubits are the natural choice for the transport of quantum information. The capability to entangle photons with trapped ions in a highly efficient (scalable) fashion is an important achievement. Here, we leverage the active and successful development of micro-fabricated semiconductor ion traps at the Sandia National Laboratory MESA facility, and integrate micro optical components. Compared to current efforts in academic settings combining macro-sized ion traps and optics, a micro device will result in the dramatically increased speed and fidelity of ion-trap based quantum networking protocols. Integrating smaller components will directly allow for a stronger quantum coherent interface between a single trapped ion and a single photon. If successful, this technology could lead to new demonstrations of fundamental physics properties and would open new avenues for scalable quantum networking architectures.

## ACKNOWLEDGMENTS

The authors would like to acknowledge Todd Barrick, Mike Descour, Javier Gallegos, Ray Haltli, Bradley Jared, Daniel Stick, Ben Thurston, and Chris Tigges for their contributions to this work.

# CONTENTS



# FIGURES



# TABLES

# NOMENCLATURE

| | |
|---|---|
| cQED | Cavity QED; Cavity Quantum Electrodynamics |
| DOE | Department of Energy |
| SNL | Sandia National Laboratories |
| AOM | Acousto-Optic Modulator |
| EOM | Electro-Optic Modulator |
| LEO | Lattice Electro Optics (company) |
| ATF | Advanced Thin Films (company) |
| RoC | Radius of Curvature |
| HR | Highly Reflective |
| UV | Ultraviolet |
| IR | Infrared |
| UHV | Ultra-High Vacuum |
| RF | Radio Frequency |
| DC | Direct Current |
| SEM | Scanning Electron Microscope |
| FSR | Free-Spectral Range |

# 1. INTRODUCTION

Atom-photon quantum networks leverage the qualities of atomic systems that make it them good quantum bits (qubits) to allow long distance transfer of quantum information. The ability to share quantum information across remote locations opens up the possibility of a distributed quantum processor over a network of quantum systems. Several few-qubit quantum processors connected in a network offer the ability to perform a large-scale quantum computation across such a distributed network of quantum nodes.

Due to their long storage and coherence times, trapped ions are a leading platform to realize a quantum computer. However, connecting remote nodes of trapped ion processors requires an efficient means of extracting quantum information from the trapped ion system. Academic labs have entangled remote ions via two-photon interference and entanglement swapping (Moehring 2007). Such a system relied upon macroscopic ion traps and the collection of the emitted photon with a large numerical aperture microscope objective.

Although high fidelities of entanglement generation are reported, such experiments rely upon technologies that do not lend themselves easily to a scalable system that is capable of hosting many ion across many nodes in a quantum network. The two issues are that the traps themselves are not a scalable technology and the success probability is many orders of magnitude below unity.

The work presented in this report detail the efforts towards addressing these issues. The first is that use of microfabricated ion traps the Sandia National Laboratories MESA facility has been successfully fabricating. Traps fabricated at the MESA facility are robust and can perform the role hosting many trapped ions as well as near-identical performance between devices.

Secondly, the use of a microscope objective for photon collection results in a low photon collection efficiency and therefore low success probability. To address this issue the work here uses a moderate to high finesse optical cavity in order to increase the collection efficiency. In such a cavity, a trapped ion will coherently couple to the cavity mode at a rate that can be comparable to that of free space modes.

# 2. DESIRED SPECIFICATIONS

We first begin with the desired specifications of our cQED device, and a brief discussion on why these specifications were chosen.

1. Demonstration of high optical quality for the cavity structure, with a finesse >3,000 at 369.5nm and a comparable finesse also at 739nm.
    a. The finesse is a measure of the quality factory of the optical resonator, and is proportional to the number of round trips inside a cavity before it is lost.
    b. The higher the finesse, the longer a photon has to interrogate the ion. However at too high a finesse, coherent oscillation between the cavity mode and ion becomes evident and the excitation no longer leaves predominantly through the cavity.
    c. The importance for both 369.5nm and 739nm is because the source for the Doppler cooling light at 369.5nm is a frequency doubled laser system at 739nm. As the 369.5nm light sent to the ion is almost exactly twice the frequency of the 739nm fundamental light (not exactly twice as AOMs are used for beam switching), the 739nm light can conveniently be used to lock the cavity. This is also useful for efficient separation of the stabilization light from the single emitted photons.
2. Low enough loss in the mirror coatings to guarantee that cavity finesse is dominated by output mirror transmission rather than scatter/absorption losses (<500ppm at all wavelengths of interest).
    a. This is important to make sure that the generated photons are delivered out of the cavity, instead of being lost while still interacting with the ion-cavity system.
3. Adequate trap-cavity integrated structures to achieve photon collection efficiency > 10%.
    a. This goal was chosen to achieve world-record photon collection efficiency for such a device.
    b. The probability of successfully creating remote entanglement scales as the square of the photon collection efficiency. A photon collection efficiency of 10% represents nearly an order of magnitude improvement in this efficiency.
4. Adequate mechanism for ion loading should be provided.
    a. Of course an ion needs to be trapped within the cavity to establish the ion-cavity interaction, but it also needs to be done cleanly, whereby the cavity mirrors are kept as clean as possible.
    b. In particular, our approach is to load an ion outside of the cavity region, and shuttle it into the cavity mode.
5. Mechanical packaging and assembly scheme to align and stabilize the optical cavity should be provided.
    a. We do not want to create an assembled device that cannot be efficiently scaled to multiple devices in the future. Thus, the assembly should be carefully planned and repeatable.
6. Development of fabrication approach that is compatible with anharmonic linear trap structures and more complex trap geometries (e.g., junctions, etc.).
    a. It is important that whatever cQED device is generated, it should be compatible with other, more traditional (local ion-ion phonon gate) ion trap quantum computing approaches.

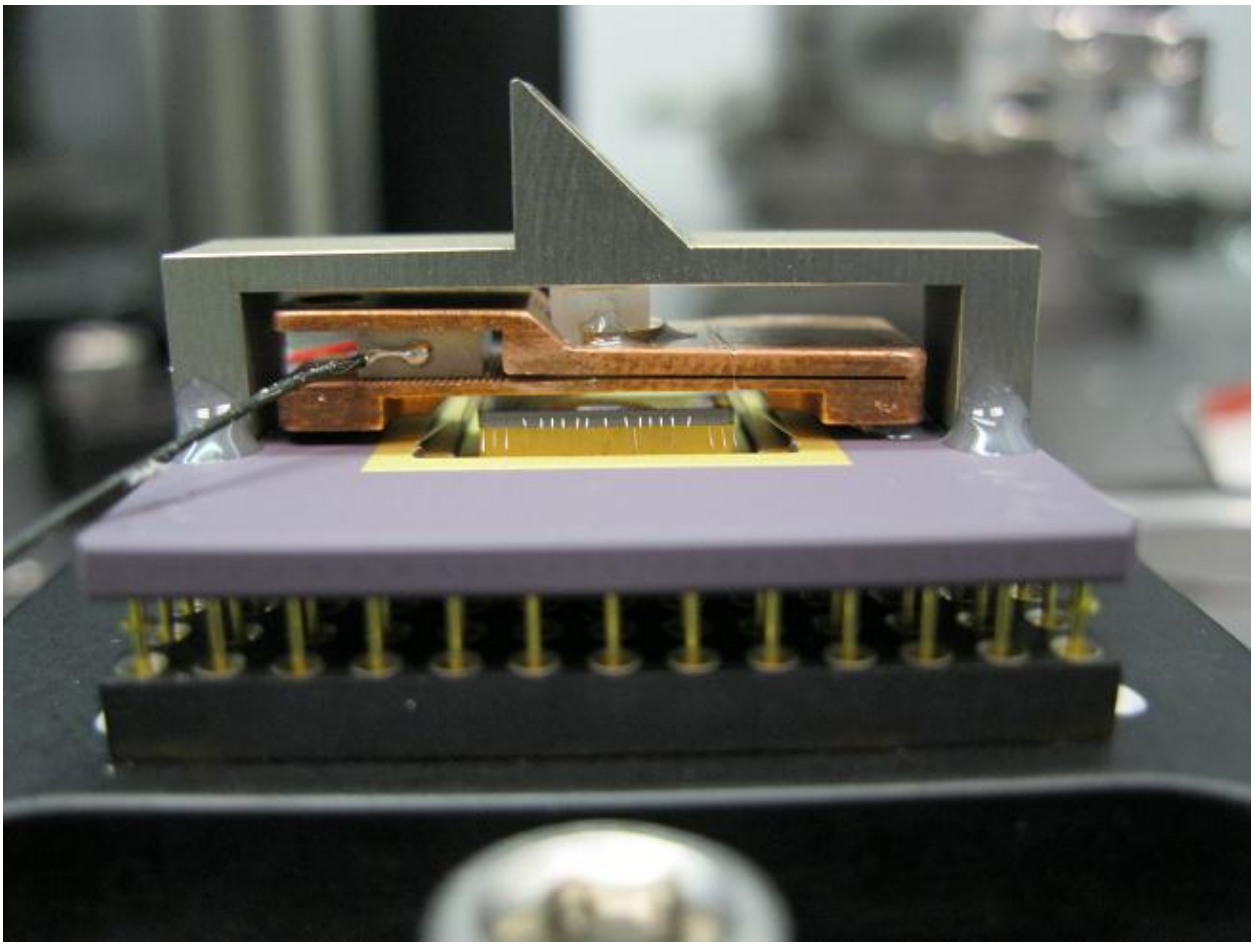

**Figure 1. Photograph of an assembled ion-cavity device before it is inserted into a vacuum chamber.**

# 3. CAVITY MIRRORS

## 3.1. Cavity Design

The cavity design begins by choosing the two mirrors that will be located on opposite sides of the ion. The image below shows the basic idea, whereby a flat mirror sits below the surface to the ion trap, and a curved mirror sits above the trap surface.

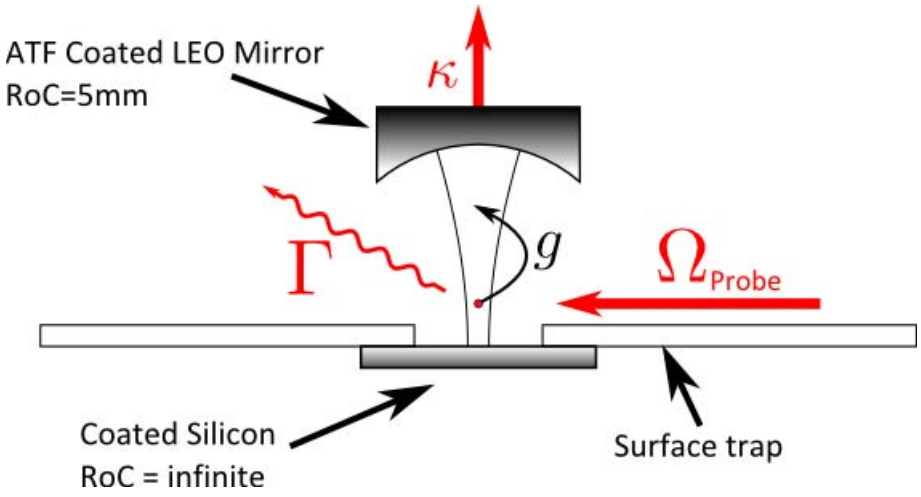


**Figure 2. Schematic of the cQED setup. The bottom mirror is a highly-reflective coated piece of silicon with an infinite radius of curvature (flat). The upper mirror is a curved mirror of 5mm RoC. The upper mirror was purchased from LEO, and both mirrors were HR coated by ATF. The ion trap has a thru hole for the cavity mode. The through-hole is 105μm in diameter, which is suitable for the 1mm long cavity mode of a 5mm RoC mirror and a flat mirror.**

As indicated in Figure 1, the curved upper mirror is also the outcoupling mirror where the photon will leave the cavity. Hence this mirror should have a higher transmission HR coating than the bottom mirror. In fact, the silicon mirror won't have transmission anyways at 369.5nm, so the upper mirror is the only choice. The mirrors are HR coated by ATF, which is essentially the only coating company in the world that will guarantee coatings with the required specifications. To design a cavity with the desired output coupling efficiency, it is important to choose the cavity length and the mirror transmissions carefully. This must take into account both the desired criteria and the realistic conditions of UV HR dielectric coatings. The collection efficiency $P_{coll}$ is given by the following equation:

$$P_{\text{coll}} = \frac{T_{\text{out}}}{\mathcal{L}} \left( \frac{2\kappa}{2\kappa + \Gamma} \right) \left( \frac{2C}{1 + 2C} \right)$$

Here, $T_{out}$ is the outcoupler transmission, $\mathcal{L}$ is the sum of all photon loss mechanisms (mirror absorption, scattering losses and transmissions), $\kappa$ is the electric field decay rate of the cavity, $\Gamma$ is the linewidth of the excited atomic state, and C is the cooperativity—the standard measure for all cQED experiments of how well coupled the cQED system is. Strong coupling is described by C>>1. Our system parameters are shown below, and also are the numerical results of our modeled system.

**Table 1. Summary of cQED design parameters**

| Parameter | Design Value |
|---|---|
| Outcoupler transmission | 1500ppm |
| Coherent coupling rate, g | $2\pi$ x 9.1MHz |
| Cavity half-width, $\kappa$ | $2\pi$ x 26.2MHz |
| Atomic linewidth, $\Gamma$ | $2\pi$ x 19.6MHz |
| Cooperativity, C | 0.16 |
| Collection Efficiency | 0.12 |
| Outcoupling efficiency | 0.68 |

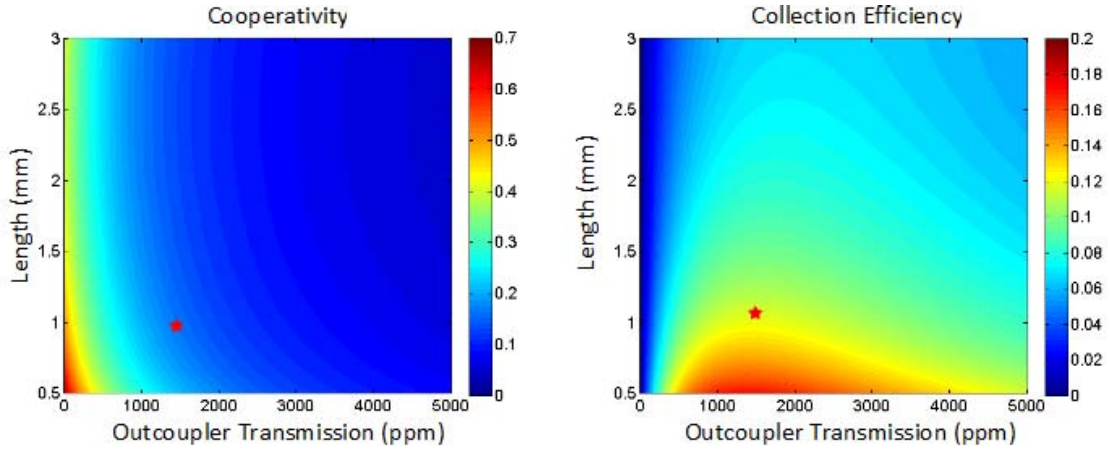


**Figure 3. Plots of the cooperativity (left) and collection efficiency (right) as a function of outcoupler transmission and cavity length. The star represents our chosen conditions.**

## 3.2. Mirror Testing

We constructed a test cavity with two LEO mirrors and measured the finesse at both 739nm and 369.5nm. The FSR of the test cavity was 95.4 GHz (hence a cavity length of 1.571mm) which was measured by scanning across adjacent resonance peaks. The full-width half-maximum of the two measured wavelengths were 5.53 M Hz at 739nm (leading to a finesse of 16,000) and 16.3MHz at 369.5nm (leading to a finesse of 5900). Both of these results were better than the requirements outlined above. The images below show important pieces of the test apparatus and the resulting data used to calculate the cavity finesse for the 739nm wavelength.

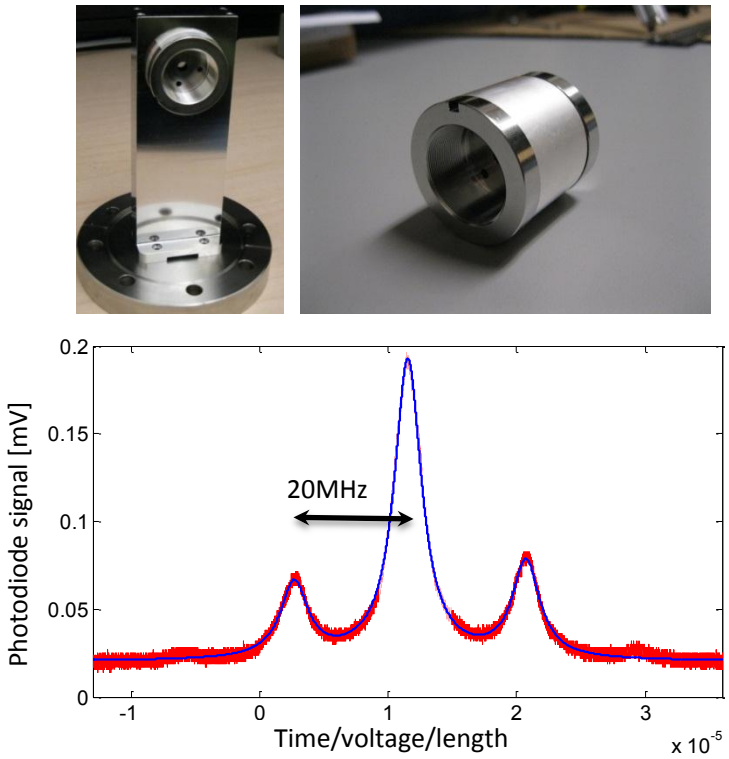


**Figure 4. Assembly for measurement of the optical coatings. Left: Apparatus for testing the cavity mirrors. The mount is connected to a UHV compatible flange for potential testing in vacuum. Center: Closer view of the mirror holding apparatus. Right: Data of the light measured through the cavity mirrors as a function of cavity length.**

The top mirror was also analyzed with a white-light interferometer. The results of this analysis are shown in the figures below, whereby it is seen that the RMS surface roughness of the LEO mirror is <1nm and has the 5mm RoC surface curvature expected. The white-light interferometer was limited to about 1nm RMS roughness as it had not been recently calibrated. The roughness on the silicon mirrors are expected to be better than 2 angstroms.

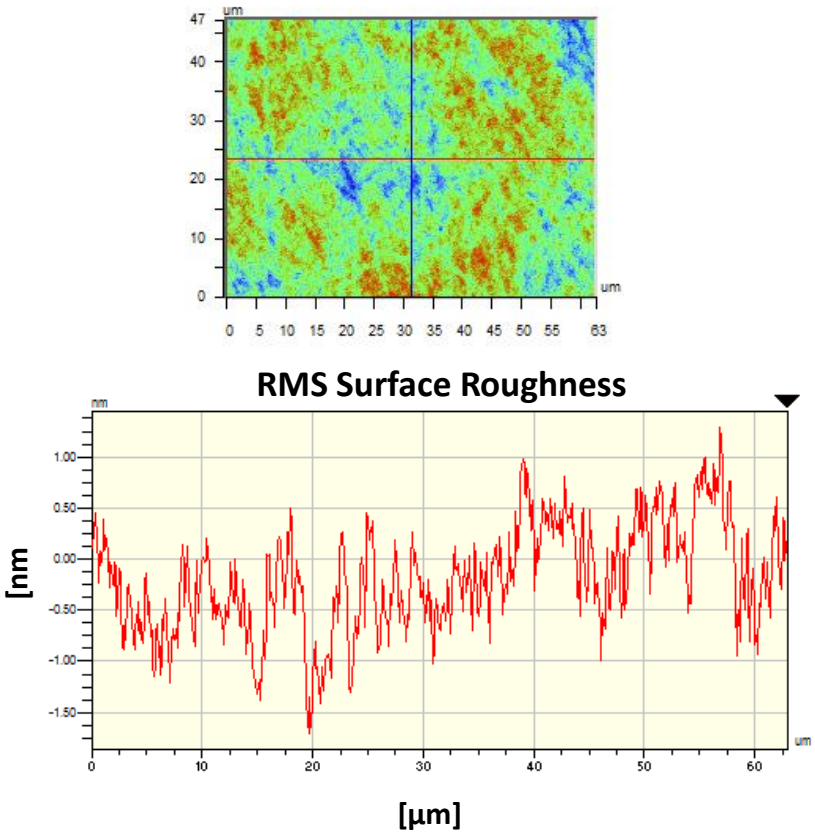


**Figure 5. Surface roughness data on the LEO mirror.**

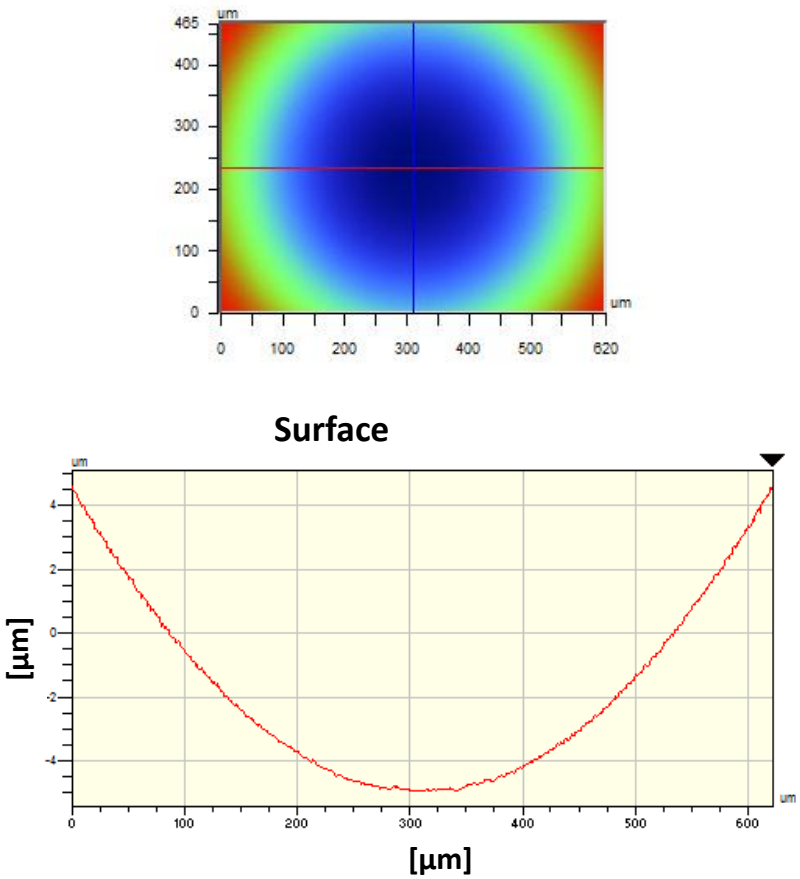


**Figure 6. Surface curvature data on the LEO mirror. The measurements show the RoC to be 5.00±0.01mm.**

## 3.3. Mirror Placement

### *3.3.1. Bottom Mirror*

The mounting of the bottom mirror is a relatively straight-forward, albeit very delicate, procedure of placing a 2mm x 2mm piece of HR coated silicon on the back of the device. The trap was backside etched in a 2.2mm x 2.2mm square shape where the mirror was inserted. Ray Haltli inserted the mirror, held it in place with a small probe, and epoxied it using UHV-compatible epoxy. The mirror placement was then analyzed with a white-light interferometer to measure the distance of the mirror below the top metal layer as well as the angle of the mirror. For the cavity mode to hit the ion, the bottom mirror must be less than 2.7° from parallel. As seen in the images below, the (first) assembled setup has <0.2µm tilt across the 105µm width. Hence, the mirror is located about 50µm below the top surface and is tilted less than 0.1 degrees.

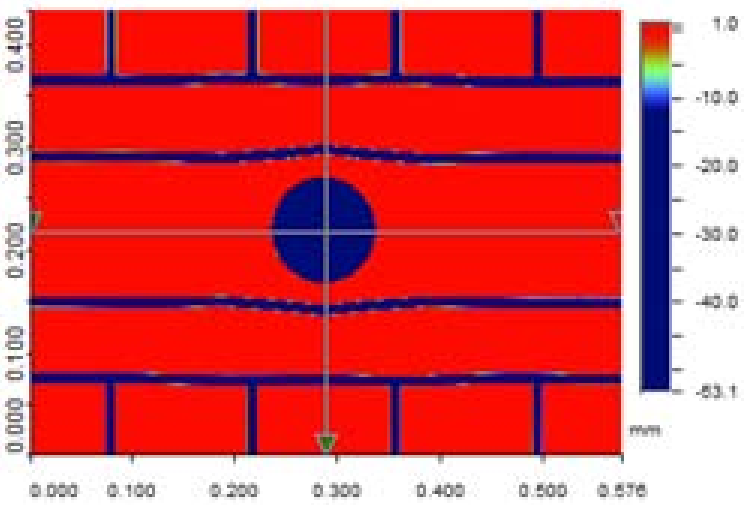


**Figure 7. White-light interferometer data on the optics hole of the ion trap with the bottom mirror inserted.**

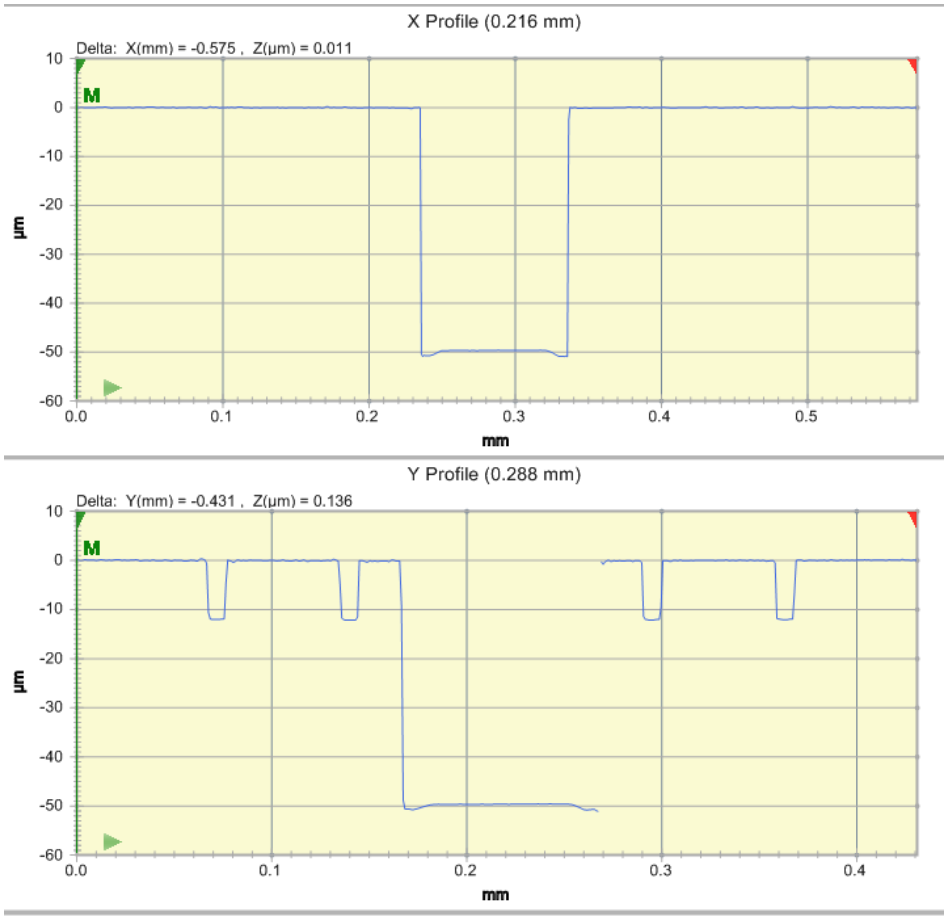


**Figure 8. White-light interferometer data from the horizontal (upper) and vertical (lower) scans of the cursor shown in the above figure.**

### *3.3.2. Upper Mirror*

The mounting of the upper mirror is a much greater challenge. This is partially due to the fact that we are mounting a bulkier mirror, but also because we need to have the ability to scan the

mirror's position vertically such that the cavity length can be locked to the optical resonance of the trapped ion. This has been accomplished using a "flexure" mount made from oxygen-free copper (good for stability and UHV compatibility) and was designed by Bradley Jared. The mirror is held in place with small drops of UHV compatible epoxy.

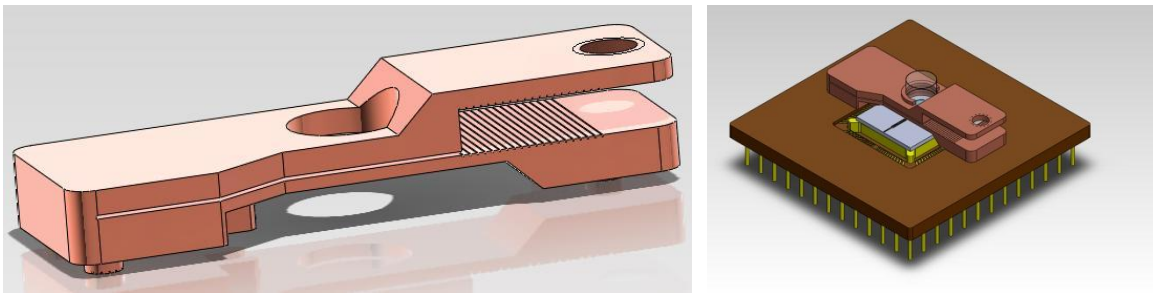

**Figure 9. Flexure mount for holding the upper mirror. Left: Solidworks diagram of the mount. Right: Solidworks diagram of how the mount will be integrated into the entire ion trap-cQED setup.**

In addition to simply knowing that the flexure mount would be capable of holding the upper mirror in the correct location, it is also important to know the mechanical resonances of the mount. The resonance needs to be sufficiently high such that it will not be a concern when trying to electronically stabilize the cavity length with the piezo. A finite element analysis of the mount (without a piezo and mirror) was performed by Bradley Jared and an optical measurement was also performed by Jonathan Sterk and Francisco Benito (with the piezo and mirror) using an interferometric setup and lock-in detection. The results below show that the lowest resonance is about 3.7kHz, sufficiently high for our purposes.

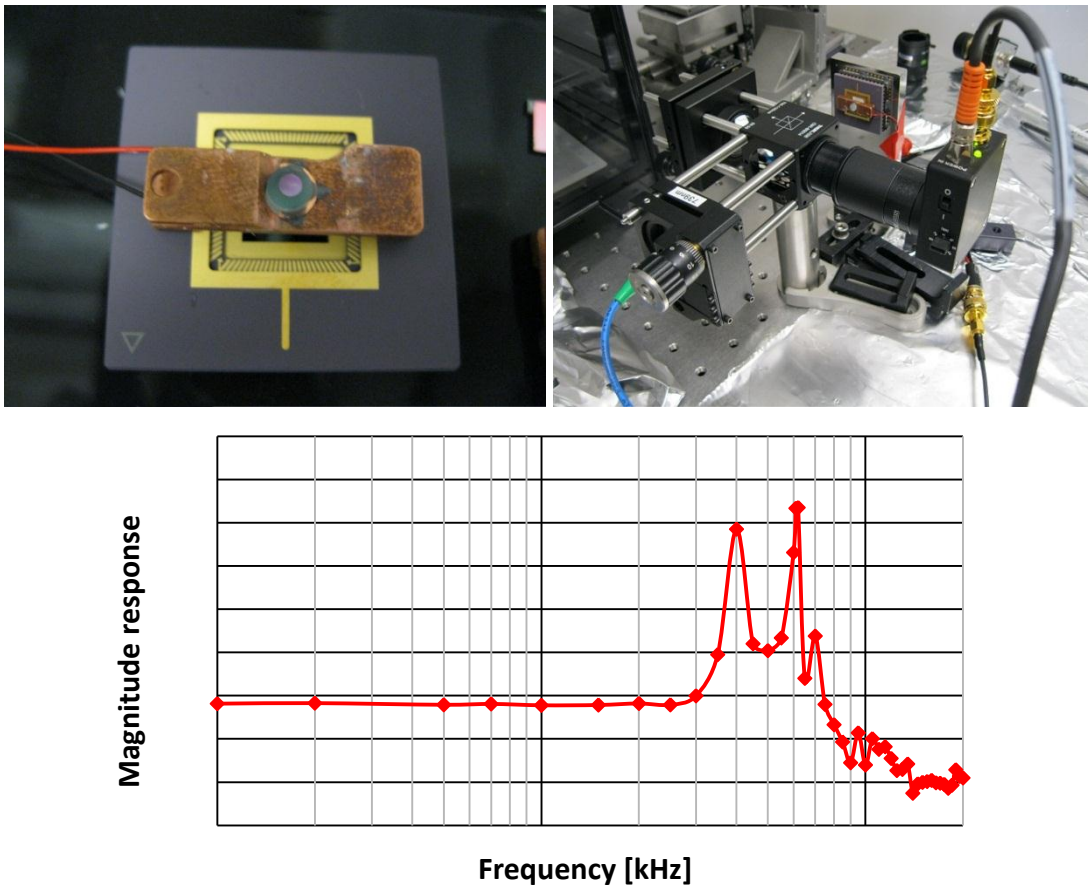


**Figure 10. Assembly for measurement of the mechanical resonance. Upper Left: The flexure mount with a mirror inserted upside-down for use in the interferometer setup. The flexure mount is attached to a CPGA for mounting purposes. Upper Right: The laser interferometer setup. Bottom: Recovery of the transfer function via lock-in detection. The lowest mechanical resonance is at 3.7kHz.**

# 4. ION TRAP

## 4.1. Trap Design

The main motivation for a new trap design was based on the desire to keep the cavity region spatially separated from the ion-loading region. The reason for this is because in order to load ions a neutral stream of atoms are sent through the trap from underneath, which can cause potential degradation of the HR mirror coatings by depositing atoms on the otherwise clean dielectric surface. As seen in the image below, this trap has been segmented into 36 pairs of DC electrodes to trap and shuttle the ions along the linear trap region. The loading hole and optics holes are separated by approximately 5mm. This separation was chosen to minimize the distance the ion would have to travel while still being large enough such that upper mirror and flexure mount would not obscure optical access to the loading hole.

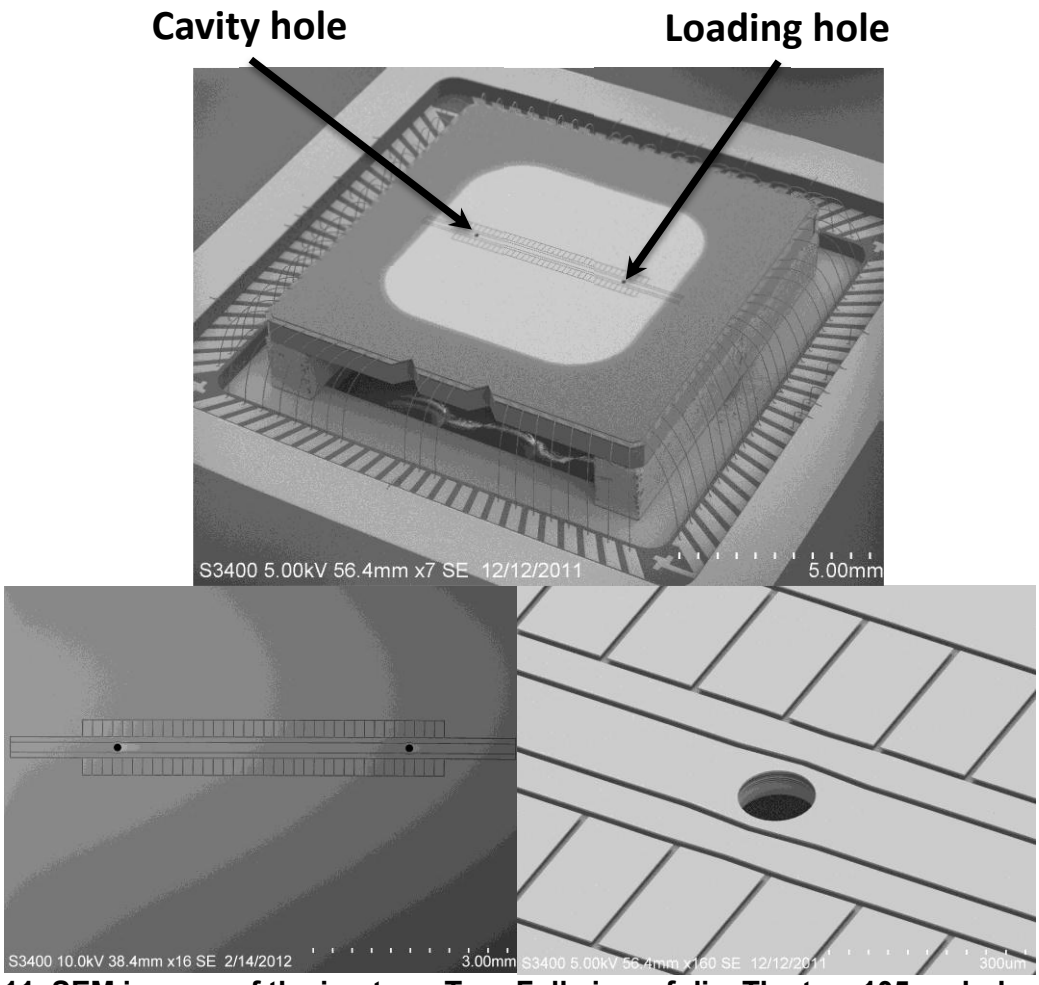


**Figure 11. SEM images of the ion trap. Top: Full view of die. The two 105μm holes for the cavity and ion loading are indicated. Bottom Left: Top view of the ion trap. Bottom Right: Zoom of one of the holes and the adjacent electrodes.**

Although the trap has 73 DC control electrodes, the trap was designed to be compatible with both 96 and 48 pin chambers. This allows the trap to be tested in any of the available ion trap test

chambers. Wiring the trap for a 48 pin chamber requires nearly all electrodes on one side of the trap to be grounded. Voltage solutions utilizing one side are referred to as „single-sided.'

In order to accurately align the flexure mount and cavity mirror assembly to the ion trap, the die was fabricated with registration notches (Figure 12. SEM image of registration notch used for alignment of the flexure mount to the ion trap.). These notches are lithographically defined and have a well-known distance from the center of the cavity hole.

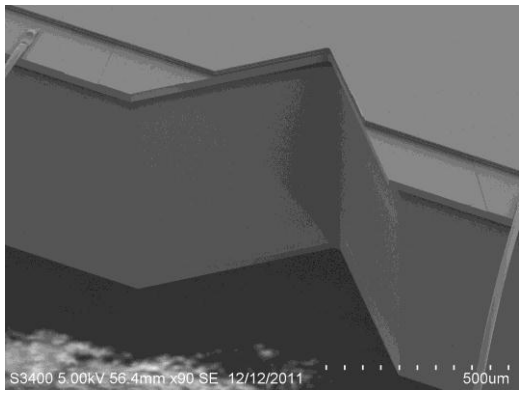


**Figure 12. SEM image of registration notch used for alignment of the flexure mount to the ion trap.**

## 4.2. Trap Results

Both calcium (mass: 40amu) and ytterbium (mass: 174amu) ions were successfully loaded in the trap with similar applied voltages. The main difference between the applied voltages was the amount of RF power needed to stably trap ions. The heavier element requires higher RF powers in order to provide a deep and strong trapping potential. Ytterbium was consistently trapped and loaded with 2 watts of RF at 34.5MHz, and could be loaded as low as 1W. Calcium ions were loaded with 1W of RF. The DC voltages for calcium and ytterbium loading were identical. Additionally these same voltages loaded ytterbium ions on a second trap, which was wired for a 48 pin chamber.

Dozens of ions were able to be loaded and shuttled across several electrodes. Single ions were shown to shuttle from one hole to the other and back. These voltage sets worked for both the 48 and 96 pin traps.

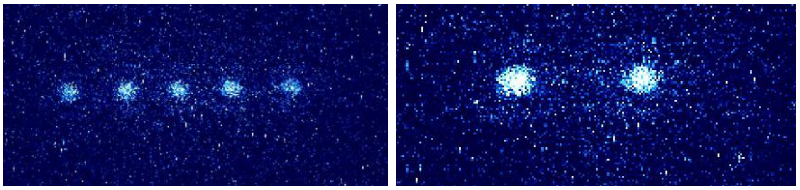

**Figure 13. Images of ytterbium ions.**

# 5. SYSTEM ASSEMBLY AND TEST

The entire system was assembled in a clean space. To assemble the system, the cavity must be aligned and the flexure mount glued in place. Although the registration notches on the trap die allow precision alignment of the flexure mount to the cavity mirror, verification of the alignment must be done with a laser coupled into the optical cavity. This allows for correct placement of the top mirror.

Laser light from a fiber passes through a collimator and a beamsplitting cube. The through beam passes through mode-matching optics and enters the optical cavity, while the reflected beam is dumped. The entire assembly is mounted on a translation stage providing fine control of the beam position. Additionally, the flexure mount assembly is attached to a translation stage as well in order for fine positioning of the top mirror. Light reflected from the cavity is sent back through the optics assembly. The fraction of light reflected from the beamsplitter is sent to either a photodiode to monitor cavity reflection or into a camera for imaging.

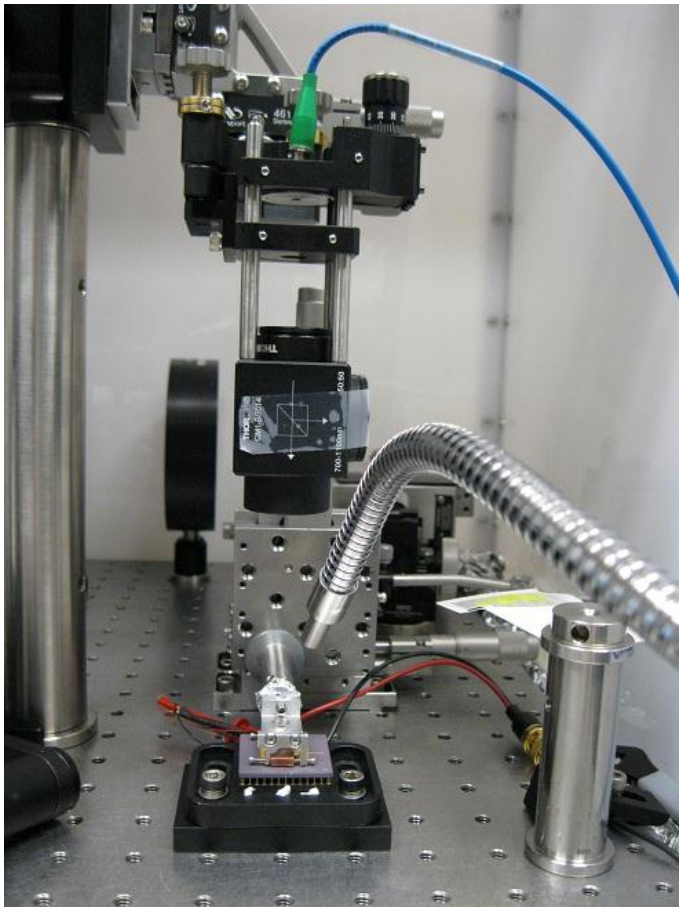

**Figure 14. Optical setup for aligning the top mirror to the ion trap.**

With the camera and a weak input beam, we were able to observe the beam spot on the ion trap surface. Using this technique we found optical modes were observable only when the spot on the trap was in the center of the bottom mirror with the reflected beam overlapping the incident beam.

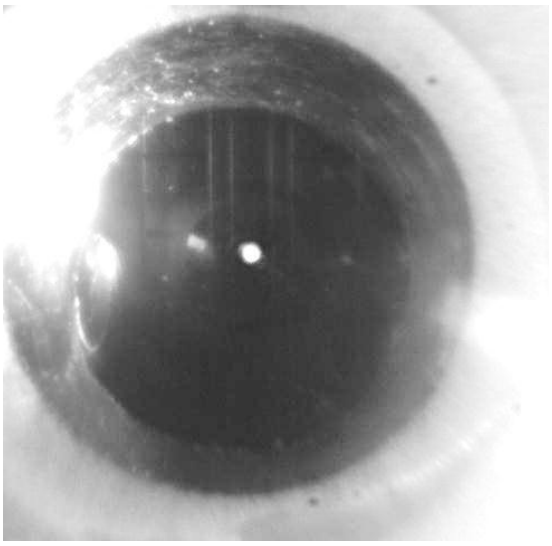

**Figure 15. Image of ion trap through top mirror during cavity aligment. The bright spot is the 739nm alignment laser reflecting off the HR silicon mirror. Electrode features are visible.**

After assembly of the ion-cQED system, it was inserted into the vacuum chamber and baked at 150°C for a couple weeks in order to reach UHV pressures. We then proceeded to load ytterbium ions in the trap. However, after a week of operation an electrical short on the RF appeared, possibly due to foreign particles on the trap acquired during cavity alignment. Nevertheless, optical modes were observed with the system under vacuum. Additionally, the cavity length was able to be stabilized.

# 6. CONCLUSIONS

We have detailed the development of an ion trap cavity system that could efficiently extract single photons from trapped ions. Utilizing the fabrication and test capabilities of SNL we have developed a microfabricated linear ion trap that can serve as simple nodes in a distributed quantum network, holding many ions. Additionally, the trap developed can serve independently of a cQED system as a traditional anharmonic linear ion trap and could serve as a testbed ion trap for verification of quantum computing procedures with trapped ions.

Although efficient photon collection has not yet been observed in the entire system, individual tests and measurements of the ion trap and optical cavity meet the design requirements indicating the system should be capable of collecting up to 12% of the emitted light. Additional work on this project will continue as part of the Multi-Qubit Coherent Operations program, funded by IARPA.

# DISTRIBUTION

| | | | |
|---|---|---|---|
| 1 | MS1071 | C. Boye | 1720 |
| 1 | MS1082 | D. Stick | 1725 |
| 1 | MS1082 | M. Blain | 1725 |
| 1 | MS1082 | C. Tigges | 1725 |
| 1 | MS1248 | S. Rinaldi | 5643 |
| 1 | MS1248 | C. Highstrete | 5643 |
| 1 | MS0899 | Technical Library | 9532 (electronic copy) |
| 1 | MS0359 | D. Chavez, LDRD Office | 1911 |


Sandia National Laboratories